JOURNAL OF MODERN OPTICS, 20 JANUARY–15 FEBRUARY 2005
VOL. 52, NO. 2–3, 261–275

Taylor & Francis
Taylor & Francis Group

Single sub-fs soft-X-ray pulses: generation and measurement with the atomic transient recorder

R. KIENBERGER†, M. UIBERACKER†, E. GOULIELMAKIS†, A. BALTUSKA†, M. DRESCHER‡ and F. KRAUSZ†§

†Institut für Photonik, Technische Universität Wien, Gusshausstr. 27, A-1040 Wien, Austria
‡Fakultät für Physik, Universität Bielefeld, D-33615 Bielefeld, Germany
§Max-Planck-Institut für Quantenoptik, Hans-Kopfermann-Straße 1, D-85748 Garching, Germany

(*Received 5 May 2004; revision received 1 Sepember 2004*)

Abstract. The change from a zero transition to the maximum amplitude of the electric field of visible light lasts shorter than one femtosecond ($1\,\text{fs} = 10^{-15}\,\text{s}$). By precisely controlling the hyperfast electric field oscillations in a short laser pulse we developed a measuring apparatus—the atomic transient recorder—like an ultrafast stopwatch. This apparatus is capable of measuring the duration of atomic processes with an accuracy of less than 100 as ($1\,\text{as} = 10^{-18}\,\text{s}$), which is the typical duration of electronic processes (transients) deep inside atoms. A 250 as X-ray pulse initiates the atomic process to be measured and the attosecond stopwatch at the same time. For the first time it is now possible with this new measuring method to observe ultrafast processes in the electron shell of atoms.

1. Introduction

Efforts to access ever shorter time scales are motivated by the endeavour to explore the microcosm in ever smaller dimensions. Recently, femtosecond laser techniques have allowed control and tracing of molecular dynamics and the related motion of atoms on the length scale of internuclear separations without the need for resolving the objects of scrutiny in space [1]. Here we demonstrate that laser light consisting of a few, well-controlled field oscillations [2] extends these capabilities—again without resolving particles in space—to the interior of atoms, allowing control and measurement of electronic motion on an atomic scale of time.

Measurement of ever shorter intervals of time and tracing of dynamics within these intervals rely on reproducible generation of ever briefer events and on probing techniques of corresponding resolution. The briefest events produced until recently have been pulses of visible laser light, with durations of around 5 fs ($1\,\text{fs} = 10^{-15}\,\text{s}$) [3, 4]. Traditionally, the fastest measurement techniques have used the envelope of these laser pulses for sampling [5]. Recently, sub-femtosecond bunching of femtosecond (>10 fs) extreme ultraviolet (XUV) light was observed in two-colour [6, 7] and two-photon [8] ionization

Journal of Modern Optics ISSN 0950–0340 print/ISSN 1362–3044 online
http://www.tandf.co.uk/journals
DOI: 10.1080/09500340412331315114

experiments and evidence of sub-femtosecond confinement of XUV emission from few-cycle-driven (ionizing) atoms was also obtained [9]. However, time-domain technique has hitherto not been capable of resolving the time structure of sub-femtosecond transients.

Here we demonstrate an apparatus that allows reconstruction of atomic processes with a resolution within the Bohr orbit time, which is around 150 as. An accurately controlled few-cycle wave of visible light takes 'tomographic images' of the time–momentum distribution of electrons ejected from atoms following sudden excitation. From these images the temporal evolution of *both* the emission intensity *and* initial momentum of freed electrons can be retrieved on a sub-femtosecond time scale. Probing primary (photo-excited or collisionally excited) and secondary (Auger) electrons yield insight into, respectively, excitation and subsequent relaxation processes. The transients can be triggered by an isolated attosecond electron or photon burst synchronized to the probing light field oscillations. The technique draws on the basic operation principle of a streak camera [10–14] (figure 1), where a light pulse generates an electron bunch having exactly the same temporal structure. Deflection of the electrons in an electric field allows reconstruction of the duration of the electron bunch. By measuring the temporal evolution of the emission intensity *and* momentum distribution of positive-energy electrons, the atomic transient recorder (ATR) [15] provides direct temporal insight into the rearrangement of the electronic shell of excited atoms on a sub-femtosecond scale.

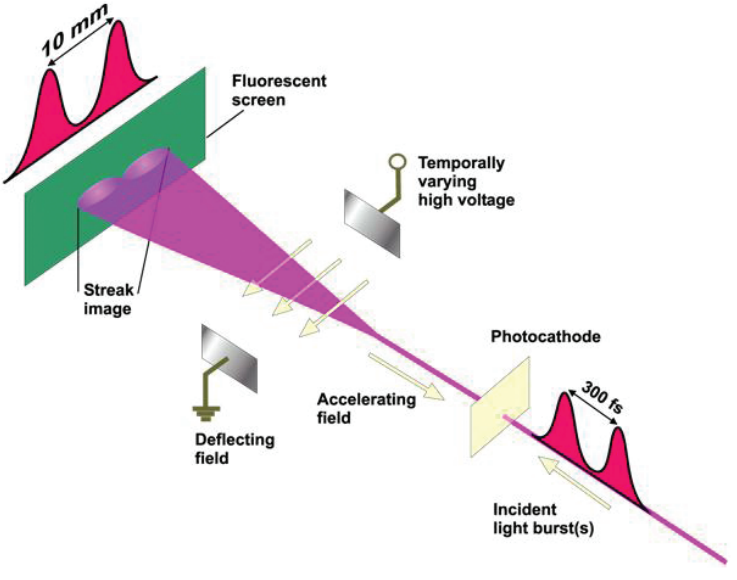

Figure 1. Principle of a conventional streak camera. In its lifetime a light flash ejects electrons from a metal plate which are then accelerated with a static electric field to a fluorescent screen. Before they hit the screen, they are deflected aside with another field increasing linearly with time. The temporally varying deflection 'streaks' the point of impact of the electrons on the screen. The spatial width of this 'streak image' (Δx) is directly proportional to the duration of the electron emission, i.e. the duration of the light flash (Δt). The faster the deflecting field varies, the shorter are the pulses that can be recorded. The most modern streak cameras attain a resolution in the region of 100 fs.

The electric field of linearly-polarized femtosecond laser pulses, if sufficiently strong, induces—in a highly nonlinear interaction—gigantic dipole oscillations by pulling an electron out of the atom and smashing it back towards its core half a cycle later. The oscillations are not sinusoidal but contain very-high-frequency components extending into the extreme ultraviolet and soft-X-ray regimes [3]. In a laser field containing many oscillation cycles, the oscillations are repeated quasi-periodically, resulting in emission of a series of high-energy bursts of sub-femtosecond duration and high-order harmonics of the laser radiation in the spectral domain. For a few-cycle laser driver only a few dipole oscillations, different in amplitude, occur. The oscillation with the highest amplitude has been predicted to produce a single burst in the spectral range of the highest emitted photon energies [2].

First evidence of emission of an isolated sub-femtosecond pulse from this interaction was reported in 2001 [9], but reproducible generation of single sub-femtosecond pulses did not become possible until giant atomic dipole oscillations could be precisely controlled with intense waveform-controlled few-cycle laser pulses in 2003 [2]. With waveform-controlled few-cycle light, the few giant atomic dipole oscillations induced can be precisely controlled and reproduced from one laser shot to the next. This is expected to result in an X-ray burst with parameters (duration, energy, timing with respect to the laser field) well reproduced from one shot to the next. This is a basic prerequisite for these tools to be used for time-resolved measurements on an attosecond time scale.

Synchronism of the X-ray burst to the field oscillations of the generating laser pulse offers the potential for using the X-ray burst *in combination with* the oscillating laser field for attosecond spectroscopy. This is essential because these laser-produced X-ray bursts are—due to the unfavourable scaling of two-photon transition cross-sections with the photon energy—too weak to be used for *both triggering and* probing electronic dynamics (X-ray-pump/X-ray-probe spectroscopy). Instead the oscillating laser field, which changes its strength from zero to maximum within some 600 as in a 750 nm laser wave, can take over the role of the probing X-ray pulse.

In the first experiments we used an X-ray excitation pulse and probed photoelectron emission, the dynamics of which yields direct information on the excitation process, namely the X-ray pump pulse. From the ATR measurements we were able to retrieve the temporal structure *and* frequency sweep of an isolated sub-femtosecond pulse for the first time. For a specific laser waveform we observe the emergence of isolated X-ray pulses with a duration of 250 as from recombination emission of atoms ionized by the few-cycle pulse. The pulses are found to carry a quadratic temporal energy sweep of several electron volts and their single-pulse structure to be sensitively dependent on the driver waveform. Our experiments have revealed that precise control of the waveform of few-cycle light is an enabling technology for both *controlling* and *tracing* atomic processes on a sub-femtosecond time scale.

2. Recording atomic transients: the development from electron-optical chronoscopy

Deflection of a light flash produces a streaked spot of the beam, allowing measurement of the flash duration [10]. Implementation of the same

concept—mapping the temporal distribution of a bunch of rapid particles to a spatial distribution by affecting their motion in a time-dependent manner—with photoelectrons allowed electron-optical chronoscopy by image-tube streak cameras [11, 12]. From the streaked image of the photoelectron bunch it is possible to infer with sub-picosecond resolution the temporal structure of the light pulse triggering the photoemission. The time resolution of these devices is ultimately limited by the spread of the electron transit time due to a spread of their initial momentum. In this work we report temporal characterization of sub-femtosecond electron emission from atoms by drawing on the same basic concept.

The three orders of magnitude improvement in time resolution results from several essential modifications of image-tube streak cameras: (i) the electric field of light is used for affecting the electrons' motion, the field (ii) is virtually jitter-free, (iii) applied along the direction of electron motion—implying their acceleration or deceleration instead of their deflection—and (iv) directly at the location and instant of emission. Whereas (i) implies 'only' a dramatically-enhanced streaking speed, the consequences of (ii)–(iv) are much more profound: (ii) allows the timing of the probing field to be systematically varied with an accuracy within the electron bunch length and, owing to (iii), this capability results in 'projecting' the initial time–momentum distribution of the electron emission into a series of different final (measurable) momentum distributions, while (iv) prevents the initial momentum spread from introducing any measurement error. As a result of (ii)–(iv), not only does the spread of initial electron momenta stop imposing a limitation on the time resolution, but also its possible temporal variation during the emission can be captured just as that of the emission intensity.

Inspired by the physics of the first sub-femtosecond experiment [9], Corkum and co-workers [13] put forward the basic concept for ATR metrology and analysed with a comprehensive quantum theory by Brabec and co-workers [14]. Let us consider electron emission from atoms exposed to a sub-fs X-ray burst in the presence of an intense, linearly-polarized, few-cycle laser field $E_L(t) = E_0(t)\cos(\omega_L t + \varphi)$. The momentum of the freed electrons is changed by $\Delta p = eA_L(t)$ along the laser field vector (figure 2). Here $A_L(t_r) = \int_{t_r}^{\infty} E_L(t)\,dt$ is the vector potential of the laser field, e and m stand for the charge and rest mass of the electron, respectively, and t_r is the release time of the electron. This momentum transfer (grey arrows in figure 3) maps the temporal emission profile into a similar distribution of final momenta $p_f = p_i + \Delta p$ within a time window of $T_0/2 = \pi/\omega_L$, if the electrons' initial momentum p_i is constant in time and their emission terminates within $T_0/2$. Under these conditions the temporal evolution of the electron emission can be unambiguously retrieved from a single 'streaked' momentum distribution. However, any sweep of the electrons' initial momentum revokes the unique correspondence between the electron's final momentum and release time, preventing retrieval of accurate temporal information from single streak records (violet and orange profiles in figure 3).

In general, the initial momentum spectrum of electrons detached from atoms by impulsive excitation varies in time during emission. A representative time–momentum distribution $n_e(p, t)$ of the electron emission rate is depicted in figure 4. The final electron momentum spectrum (observed after the laser pulse has left the interaction region), $\sigma(p) = \int_{-\infty}^{\infty} n_e(p, t)\,dt$, can be viewed as the projection of the time-dependent momentum distribution on the momentum space along

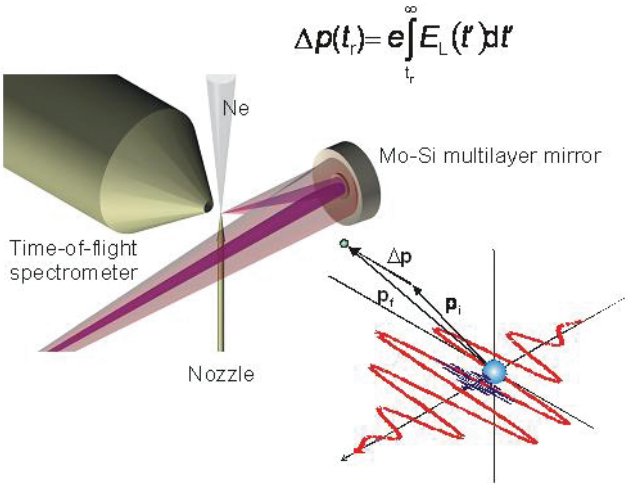

Figure 2. Light-field-controlled streak camera. The red and the blue curves represent, respectively, the evolutions of the electric field of the laser light and the intensity of the attosecond X-ray flash. Both pulses are focused into a gas target by a multilayer mirror. The X-ray pulse excites the atoms, which then emit electrons. The electrons ejected in the direction of the electric field of the laser light pulse simultaneously beamed in are detected. They undergo, depending on the time of their emission within half the oscillation period of the laser light, a change of velocity which is measured by a time-of-light spectrograph.

the lines of constant p. In the classical description of the freed electrons' motion in the strong laser field, the final spectra obtained in the presence of a strong laser field are generalized projections along the lines where $p_f = p_i + eA_L(t)$ is constant (see figure 4). By delaying the laser field with respect to the the excitation that triggers electron emission, we obtain a set of tomographic records (briefly: streaked spectra),

$$\sigma_A(p) = \int_{-\infty}^{\infty} n_e(p - eA_L(t), t)\,dt\ , \tag{1}$$

from which, with a suitable set of $A_L(t - \Delta t_n)$, the complete distribution $n_e(p, t)$ can be reconstructed. The maximum energetic shift of the photoelectron spectra reveals not only the position of the maxima (and other extreme values) of the vector potential A_L but also their magnitudes.

The method is closely related to frequency-resolved optical gating [15–19] with the oscillating field as gate and other concepts of tomography for ultrashort pulse measurements [20–22]. In the simplest cases two streaked spectra (in addition to the field-free spectrum) may be sufficient. In the absence of a nonlinear momentum sweep the streak records obtained near the zero transitions of $A_L(t)$ with opposite slopes (violet profiles in figure 3) together with the field-free spectrum (black profile) allow determination of all relevant characteristics: the temporal profile, duration and momentum chirp of emission. Note that a linear momentum sweep leads to asymmetric broadening of the streaked spectra at these delays and it is this asymmetry that makes the measurement highly sensitive

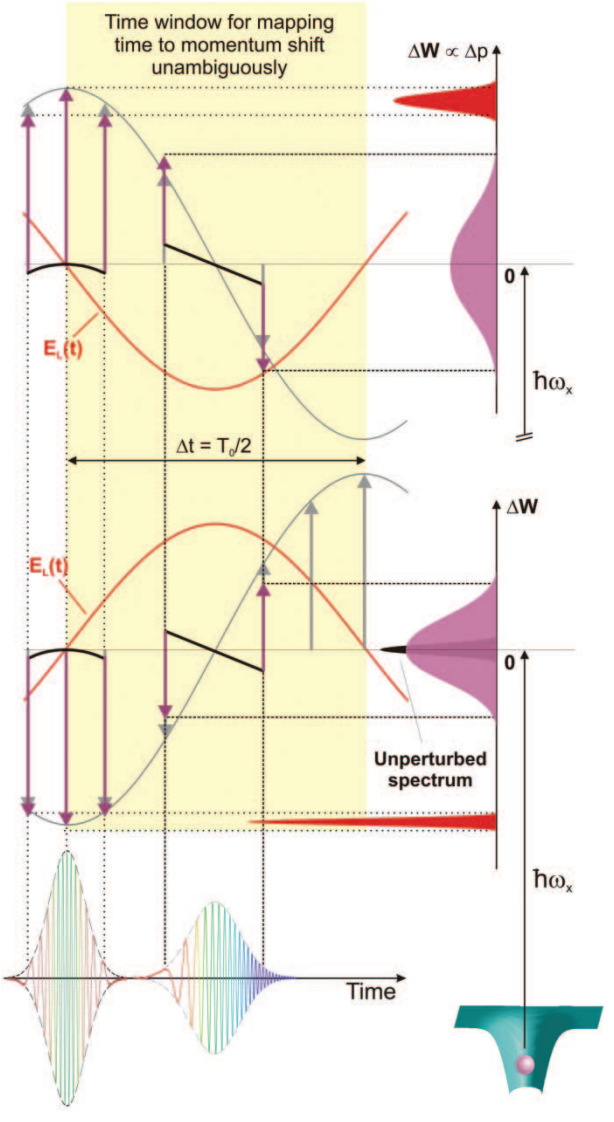

Figure 3. Streaked (violet) and shifted (orange) spectra in specific cases. In the absence of a momentum sweep of the emitted atomic electrons, $n_e(p_i, t) = f(p_i)g(t)$, the momentum transfer $\Delta p = eA_L(t_r)$ (grey lines) would map the temporal emission profile $g(t)$ uniquely into a similar distribution of final momenta. In this case the temporal intensity profile of the electron emission is directly mirrored by the streak record just as in a conventional streak camera. However, any sweep of the electrons' initial momentum (e.g. a linear one as indicated by the rainbow-ordered colours) revokes the unique correspondence between the electron's final momentum and release time, preventing retrieval of accurate temporal information from single streak records. In this case, at least two streak records (violet profiles)—in addition to the field-free spectrum (black profile)—are required. At the maximum and minimum of the vector potential of the field $A_L(t)$ the final momentum distributions are up- and downshifted, respectively (orange profiles). The different shapes of the final momentum distributions indicate the ATR's power to determine all relevant characteristics of the X-ray pulse. A high-order momentum sweep, e.g. caused by a quadratic chirp of the X-ray pulse (indicated by the red–green–red colour profile), can easily be recognized.

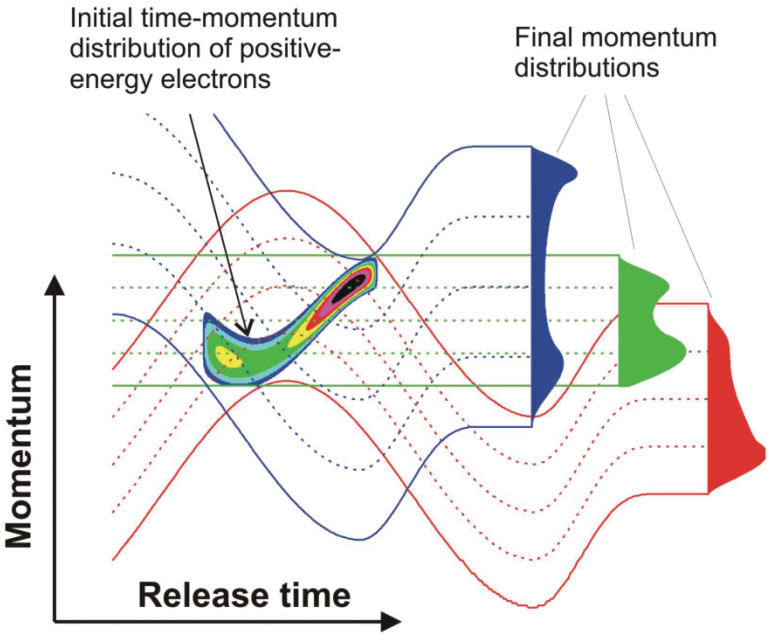

Figure 4. Time-dependent momentum transfer to positive-energy electrons within the laser cycle. Electrons emitted from an excited atom along the electric field vector of a strong laser field with an initial momentum p_i suffer a momentum change that is proportional to the vector potential of the field $A_L(t)$ at the instant of release. If electrons with a constant initial momentum (distribution) are emitted and the process terminates within less than half a laser cycle $T_0/2$, the sub-femtosecond temporal intensity profile of emission (green profile) is mapped into a similar final momentum distribution (grey profile) measurable after the laser pulse has left the interaction region. This time-to-momentum mapping is unique and allows retrieval of the temporal emission profile from the momentum distribution in a single 'streak camera' measurement only in the absence of a momentum sweep of the emitted electrons. For instance, a linear momentum sweep ('chirped' emission, rainbow profile) leads to different final momentum distributions for $A_L(t)$ with a positive and a negative slope, respectively, and can be most sensitively observed in the streaked spectra recorded near the zero transitions of $A_L(t)$ (violet profiles).

to the momentum sweep, i.e. highly sensitive to deviations of the pulse duration from the Fourier limit.

The ATR's potential for determining a high-order chirp of the X-ray pulse, too, is indicated by the different shapes of the orange momentum distributions in figure 3.

3. Experimental set-up

Using the experimental set-up described in [9] and recently employed for probing Auger electrons on a few-femtosecond time scale [23], we sample electron emission from atoms. The essential innovation here is that waveform-controlled few-cycle light now provides a reproducible excitation burst for accurate triggering and a reproducible streaking field for capturing sub-fs electron emission from atoms. For excitation, X-ray bursts are produced from Ne atoms ionized by intense, few-cycle waveform-controlled light pulses [2] in a process giving rise

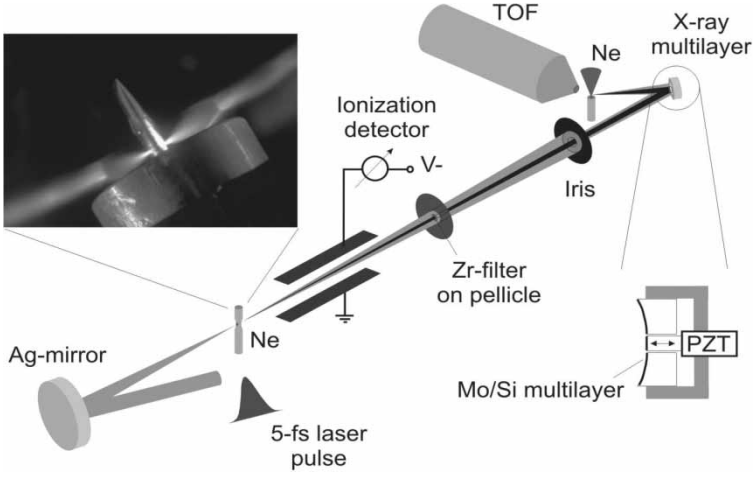

Figure 5. The schematic of the experiment. The focused 5 fs laser beam interacts with neon atoms to produce high-harmonic radiation. The laser and the highly collimated X-ray beam co-propagate collinearly through a 2 m beam line towards the measurement. Differential pumping stages reduce the pressure from $\sim 4 \times 10^{-2}$ mbar in the source chamber to the range of $\sim 10^{-5}$ mbar in the experimental chamber. An ionization detector in the higher-pressure part of the beam line serves for monitoring the (spectrally integrated) high harmonic flux. In the beam line the laser and harmonic beams pass through a 200 nm thick, 3 mm diameter zirconium foil placed on a 5 µm thick nitrocellulose pellicle to cover a hole 2 mm in diameter. The energy transported by the resulting annular beam can be adjusted with a motorized iris between a fraction of a microjoule and a few tens of microjoules. The Mo/Si multilayer consists of an annular part having an outer diameter of 10 mm with a concentric hole of 3 mm diameter hosting a miniature mirror of slightly smaller diameter. Both parts originate from the same substrate, ensuring identical radii of curvature ($R = 70$ mm). The miniature central mirror is mounted on a quadrant piezo stage, allowing alignment and translation with respect to the external part.

to high-order harmonics of the incident light for periodic (multi-cycle) pumping [24, 25]. The X-ray pulses exciting the neon harmonic source co-propagate with the laser pulses down the beam delivery tube (figure 5). After 150 cm they hit a 200 nm thick zirconium foil with an aperture of 2 mm mounted on a nitrocellulose membrane 5 μm thick. This virtually dispersionless filter produces an annular laser beam with the X-ray beam in the centre. The energy in the laser beam is adjusted by a motorized iris and measured by a photodiode. The collinear X-ray and laser beams are focused into a neon gas jet and delayed with respect to each other for the ATR measurements with a two-component Mo/Si broadband multilayer mirror (radius of *curvature* $= -70$ mm) placed 2.5 m downstream from the source. This mirror is mounted on a motorized stage so that it can be removed from the beam line. In this way the harmonic beam can be detected by an X-ray charge-coupled device (CCD) camera for optimizing the radial intensity profile of the X-ray beam (by fine adjustment of the position and pressure of the neon gas target and of the intensity of the laser pulses). Further on, a transmission grating having 10 000 lines mm^{-1} can be inserted before the X-ray CCD camera to observe the spectrum of the harmonic radiation. Fine tuning of the cut-off of the X-rays can be carried out by fine tuning of the energy of the fundamental laser beam. The reflectivity band of the multilayer extends from

85 to 100 eV with a peak reflectance of ~30% and a full width at half maximum (FWHM) of ~9 eV.

Two types of experiments based on the ATR concept were implemented. First, we used the internal part of the Mo/Si mirror to focus both the X-ray and the laser beam to eliminate any external source of fluctuations in the timing between the excitation and probing pulses. In the second type of studies, the X-ray and the laser beam were reflected by different sections of the focusing mirror: the central piece sits on a piezo stage adjustable in the transverse and longitudinal directions. In this manner the two pulses can be overlapped spatially and temporally in the focal plane, exactly where the tip of a nozzle emitting the atoms to be photoionized is placed. Electrons ejected following the X-ray excitation are collected within a narrow cone ($<4^\circ$) aligned parallel to the laser and X-ray polarization and analysed with a time-of-flight spectrometer. In these investigations the probing laser field could be delayed with respect to the X-ray excitation pulse by translation of the internal part of the mirror on a nanometre scale.

The profile of the laser focus is imaged by a lens on a CCD camera for monitoring and course pre-adjustment of the spatial overlap between the beams reflected by the two components of the Mo/Si mirror.

4. Generation of an isolated single sub-fs X-ray excitation pulse

Figure 6 summarizes representative results of a series of measurements of streaked X-ray photoelectron spectra recorded with the X-ray and laser pulse impinging with a fixed relative timing set in the X-ray generation process. According to an intuitive one-active-electron model of Schafer *et al*. [26, 27], Corkum [28] and Lewenstein *et al*. [29] ionization of atoms by a linearly polarized laser field is accompanied by emission of extreme ultraviolet radiation due to recombination of the detached electron into its original ground state upon recollision with the parent ion. These theories along with a number of numerical simulations [29–34] predict emission of the highest-energy (cut-off) photons to occur near the zero transition(s) of the electric field following the most intense half cycle(s) at the pulse peak in a few-cycle driver.

In a cosine waveform ($\varphi = 0$) cut-off emission is expected to be confined to a single bunch emitted at the zero transition of $E_L(t)$ following the pulse peak. The photoelectrons ejected in the direction of the peak electric field at this instant suffer maximum increase of their momentum and hence of their energy. The streaked spectrum in figure 6 (*d*), obtained with 5 fs, 750 nm cosine pulses used for both X-ray generation and subsequent electron streaking, corroborates this prediction. The photoelectron spectrum peaking at $\hbar\omega_{\text{x-ray}} - W_b \approx 72$ eV (where $\hbar\omega_{\text{x-ray}} \approx 93.5$ eV is the centre of the X-ray spectrum selected by the Mo/Si mirror and $W_b = 21.5$ eV is the binding energy of the most weakly bound valence electrons in Ne) in the absence of the laser field is upshifted by several 10 eV with only a few electrons scattered outside the shifted band. The clear upshift is consistent with the X-ray burst coinciding with the zero transition of the laser electric field (see figure 6 (*d*)). Possible satellites would appear at the adjacent zero transitions of $E_L(t)$ and suffer an energy downshift. The absence of a downshifted spectral peak of substantial intensity indicates clean single sub-fs pulse generation.

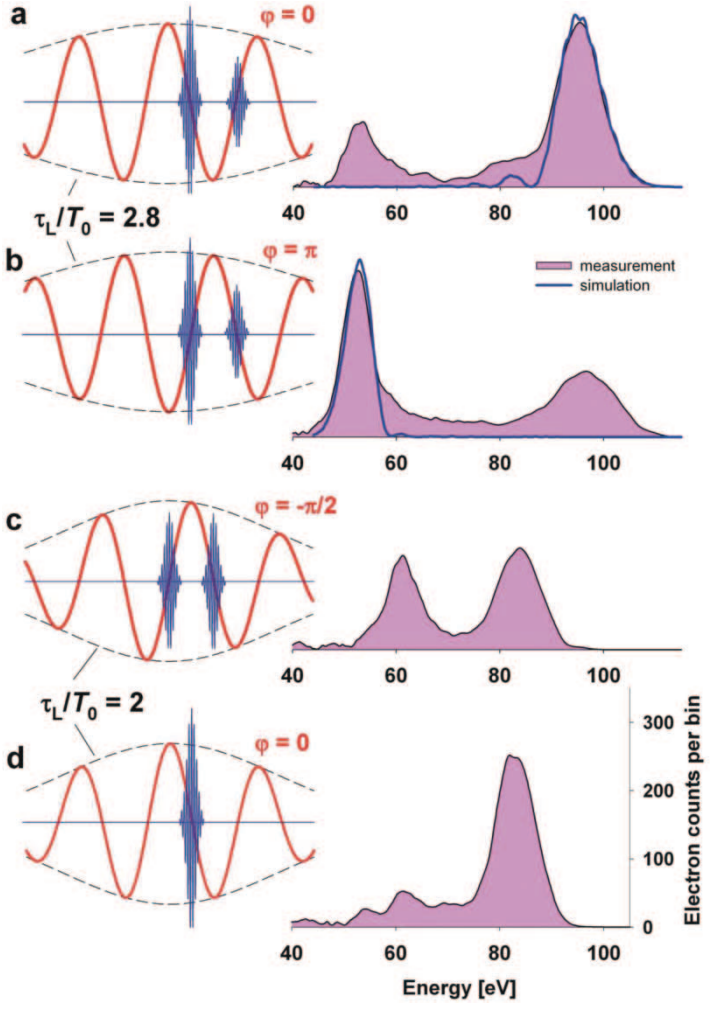

Figure 6. Streaked photoelectron spectra recorded at a fixed delay of the probing light. Energy distribution of photoelectrons emitted from neon atoms excited by a sub-fs X-ray pulse carried at a photon energy of ≈93 eV. The X-ray bursts (blue lines on the left-hand side) originate from the spectrally filtered cut-off energy range of recombination emission from another target of neon atoms pumped by intense few-cycle 750 nm laser pulses (red lines); (*a*), (*b*) streaked spectra obtained with laser pulses with a normalized duration of $\tau_L/T_0 = 2.8$ having a cosine and a −cosine waveform, respectively. The blue lines on the right-hand side depict calculated spectra obtained on the assumption of zero spectral phase (Fourier-limited X-ray burst). The calculations do not model the satellite pulse because the corresponding modulation of the (unperturbed) photoelectron spectrum is insufficiently resolved. However, the asymmetric broadening is well accounted for. (*c*), (*d*) Streaked spectra obtained with laser pulses with a normalized duration of $\tau_L/T_0 = 2$ having a sine and cosine waveform, respectively.

With the phase adjusted to yield a sine waveform ($\varphi = -\pi/2$), cut-off emission is predicted to come in twin pulses (blue line in figure 6 (*c*)) [2]. Observation of the double-peaked streaked spectrum (figure 6 (*c*)) clearly reflects this time structure. Instead of being confined to a single burst the filtered high-energy X-ray photons

are now distributed in two bursts, each of which is less than half as intense as the isolated burst produced by the cosine waveform (figure 6(*d*)). These measurements demonstrate how control of the waveform of few-cycle laser light allows one to control the temporal profile of X-ray emission within the half wave cycle, i.e. on a sub-femtosecond time scale.

For generation of a single sub-fs X-ray burst a crucial role is played by the normalized pulse duration τ_L/T_0 other than the carrier-envelope phase φ. This is demonstrated by repeating the measurements with, slightly longer, 7 fs laser pulses ($\tau_L/T_0 = 2.8$). The corresponding streaked spectrum obtained for $\varphi = 0$ (figure 6(*a*)) exhibits a sizeable downshifted spectral feature in addition to the upshifted main peak, indicating the appearance of a substantial satellite pulse (≈30% of the principle burst) in the cosine-wave-driven recombination emission. A reduced difference in intensity of the adjacent half cycles of the few-cycle wave implies that the highest-energy spectral components of adjacent bursts reach the energy band selected by our 15%-bandwidth bandpass filter. Shifting φ by π results in the same emission but the streaking is reversed (figure 6(*b*)). In these measurements (figure 6(*a*) and (*b*)) we increased the strength of the streaking laser field by a factor of approximately 2. The increased streaking reveals pronounced asymmetry of the up- and downshifted spectra, which is consistent with a near-quadratic temporal energy sweep of the X-ray burst. This results from the asymmetric spectral intensity profile filtered by the Mo/Si mirror. The (near) quadratic momentum sweep of the electron emission yields asymmetric streaking at the adjacent maxima of $A_L(t)$ in a way similar to that of a linear chirp at subsequent zero transitions of $A_L(t)$.

5. Measurement of the time–momentum distribution of atomic electron emission

With isolated sub-fs X-ray pulses at our disposal atomic transients can now be triggered and their subsequent evolution be captured by probing electron emission with a synchronized wave of laser light. In the first ATR measurements presented here, the objects of scrutiny were photoelectrons. The streaking field in these experiments was produced by blocking the internal part of the laser beam with a zirconium filter (transmitting the X-ray pulse) and focusing the transmitted annular beam on the target with the external section of the Mo/Si mirror [9], which can be delayed with respect to the internal section that focuses the X-ray beam. Figure 7 shows a series of streaked spectra of photoelectrons emitted from neon as a function of Δt. The excitation pulse at 93 eV was produced by a cosine waveform with $\tau_L/T_0 = 2$.

If the electrons are emitted with an initial kinetic energy much larger than their average quiver energy in the laser field and temporally confined to a fraction of the half oscillation cycle, theory predicts that their energy shift is linearly proportional to Δp and hence to the vector potential at the instant of release of the wavepacket, $\Delta W(t_r) \approx (p_i/m)\Delta p(t_r) = (ep_i/m)A(t_r)$, where p_i is the initial momentum of the electron. As a consequence, $A_L(t)$ and hence $E_L(t)$ can be accurately determined from the peak shifts of the spectra—without having to analyse their detailed structure. The result is shown by the black line in figure 7, constituting the first direct (time-resolved) measurement of a visible light field. From this measurement we can also evaluate the half oscillation period of the electromagnetic field

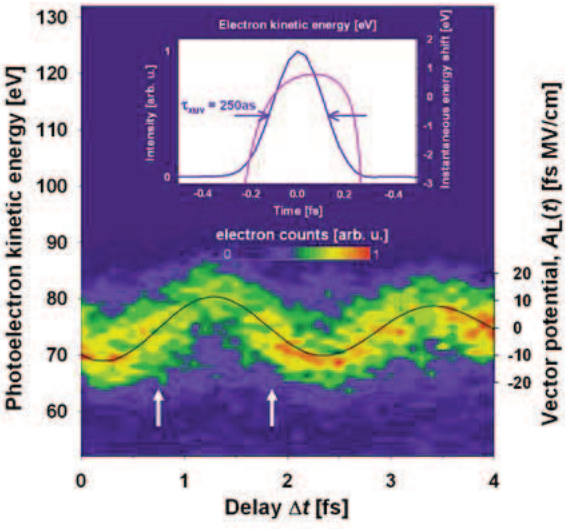

Figure 7. ATR measurement: a series of tomographic projections (streaked kinetic energy spectra) of the initial time–momentum distribution of photoelectrons ejected by a single sub-fs X-ray pulse (in false-colour representation). A few-cycle laser pulse with a cosine waveform and a normalized duration of $\tau_L/T_0 = 2$ was used for both generating the single sub-fs excitation pulse and probing photoelectron emission in the atomic transient recorder. Black line: $A_L(t)$ of the probing field evaluated from the peak shift of the streaked spectra (see scale on the right-hand side). Inset: temporal intensity profile and energy sweep of the sub-femtosecond X-ray excitation pulse evaluated from the ATR measurements. The basis of the calculation was the unperturbed and two streaked spectra at the zero transitions of the laser electric vector potential marked by the two white arrows.

as $T_0/2 \approx 1$ fs. This latter value indicates a significant blueshift to a carrier wavelength of 600 nm near the pulse peak (origin: ionization-induced self-phase modulation in the X-ray source), in agreement with previous observations [9]. With the streaking field $A_L(t)$ known, full temporal (time–momentum) characterization of sub-femtosecond electron emission is now becoming feasible. This capability strictly relies on light waveform control: in its absence the streak records smear out beyond redemption due to irreproducible excitation and probing.

First, we are interested in a possible linear frequency sweep carried by the X-ray pulse, because this tends to have a dominant effect on the shape and duration of the excitation. To this end, we analysed streaked spectra recorded at adjacent zero transitions of $A_L(t)$ (indicated with white arrows in figure 7). Streaked spectra recorded at these instants are most sensitive to a linear momentum sweep (caused by a linear frequency sweep of the X-ray pulse), as shown in figure 3. By assuming possible spectral phase modulation of $\phi_{x\text{-}ray} = \beta_2(\omega - \omega_{x\text{-}ray})$ [2] carried by the X-ray pulse and allowing for a timing jitter between the X-ray pulse and the streaking field, we evaluated $\tau_{x\text{-}ray} = 250(-5/+30)$ as and $\tau_{jitter} = 260(\pm 80)$ as from the best. The relatively large jitter is likely to originate from mechanical vibrations introduced by the vacuum pumps, suppression of which is under way. The temporal intensity profile and chirp of the X-ray pulse obtained from the ATR measurements are shown in the inset of figure 7. The pulse is found to be essentially Fourier-limited (the near-quadratic frequency sweep results from the asymmetric shape of the pulse spectrum rather than

from a spectral phase). The remarkable accuracy of $\tau_{\text{x-ray}}$ relies on using several (in this case 3) tomographic projections of the time–momentum distribution of photoelectrons for the X-ray pulse retrieval, which is the essence of the ATR concept. Restricting our analysis to only one of the two streaked spectra—in the spirit of streak camera measurements—would only allow setting an upper limit of 500 as on the X-ray pulse duration. Extension of this analysis to a series of spectra measured within a delay range of T_0 revealed the absence of higher-order contributions to $\tau_{\text{x-ray}}$ as well. These measurements provide evidence of the emergence of isolated, bandwidth-limited X-ray bursts over a relative spectral band as broad as 15% (15 eV at 100 eV) from recombination emission driven by a cosine waveform with $\tau_L/T_0 = 2$. This has important implications for scaling the technology.

6. Resolving atomic transients within the Bohr orbit time

Quantum mechanical uncertainty, which dictates that any short time structure comes with a broad energy spectrum, limits the briefest time interval within which two different atomic events can be recognized as different by our apparatus. To be able to resolve the spectral 'images' of two events separated by δt in time they must be shifted with respect to each other in the streak record by at least as much as their own spectral width $\delta W \approx \hbar/\delta t$. From this requirement we obtain the ATR resolving power as

$$\delta t = \frac{T_0}{2\pi}\left(\frac{\hbar\omega_L}{\Delta W_{\max}}\right)^{1/2}, \tag{2}$$

where $\Delta W_{\max}$ stands for the energy shift suffered by the electron ejected at the peak of $A_L(t)$. Under our current experimental conditions $\Delta W_{\max}$ can exceed 20 eV (see figures 6 (*a*) and (*b*)) before the onset of laser-induced ionization, yielding (for $T_0 = 2$ fs) $\delta t \approx 100$ as. The atomic transient recorder driven by a 600 nm wavelength light field and probing electrons with a kinetic energy near 100 eV is able to distinguish two ultrafast atomic events following each other within 100 as, constituting the shortest interval of time directly measurable to date.

Our experiments indicate that there is room for further improvement. The absence of spectral phase modulation in the cut-off energy range of few-cycle driven recombination emission over an energy band as broad as 15% and the confinement of this emission to a single burst afford promise of the generation of single 50 as pulses from the same source upscaled to photon energies of 500 eV [35]. At these excitation energies $\Delta W_{\max}$ can be enhanced by at least an order of magnitude, yielding $\delta t \approx 30$ as. Extension of the experiments presented to exploring of the sub-femtosecond temporal variation of the emission intensity and momentum distribution of primary (photo) *and* secondary (Auger) electron emission simultaneously will provide unprecedented insight into the excitation and relaxation dynamics of the electronic shell of atoms and molecules. The currently used time window of $T_0/2 \approx 1$ fs can be extended to several 10 fs by difference frequency generation with the few-cycle laser pulse whilst keeping the resolution of the ATR in the sub-fs regime. At near-keV excitation energies, the atomic transient recorder presented here will allow time-domain metrology of atomic dynamics with a resolution approaching the atomic unit of time (24 as).

Acknowledgments

We gratefully acknowledge the invaluable contributions of V. Yakovlev, F. Bammer, A. Scrinzi, Th. Westerwalbesloh, U. Kleineberg and U. Heinzmann to the experiments reviewed in this paper. Sponsored by Fonds zur Förderung der wissenschaftlichen Forschung (Austria, grants Z63 and F016), Deutsche Forschungsgemeinschaft (Germany, grants SPP1053, HE1049/9, and KL1077/1) and the European Union's Human Potential Programme under contract HPRN-2000-00133 (Atto). R. Kienberger is funded by an APART fellowship of the Austrian Academy of Sciences.

References

[1] Zewail, A., 2000, *J. phys. Chem.* A, **104,** 5660.
[2] Baltuska, A., Udem, Th., Uiberacker, M., Hentschel, M., Goulielmakis, E., Gohle, Ch., Holzwarth, R., Yakovlev, V. S., Scrinzi, A., Haensch, T. W., and Krausz, F., 2003, *Nature,* **421,** 611.
[3] Brabec, T., and Krausz, F., 2000, *Rev. mod. Phys.,* **72,** 545.
[4] Keller, U., 2003, *Nature,* **424,** 831.
[5] Drescher, M., Hentschel, M., Kienberger, R., Tempea, G., Spielmann, Ch., Reider, G. A., Corkum, P. B., and Krausz, F., 2001, *Science,* **291,** 1923 (published online 15 February 2001; 10.1126/science.1058561).
[6] Paul, P. M., Toma, E. S., Breger, P., Mullot, G., Augé, F., Balcou, Ph., Muller, H. G., and Agostini, P., 2001, *Science,* **292,** 1689.
[7] Mairesse, Y., de Bohan, A., Franinski, L. J., Merdji, H., Dinu, L. C., Monchicourt, P., Breger, P., Kovacev, M., Taïeb, R., Carré, B., Muller, H. G., Agostini, P., and Salières, P., 2003, *Science,* **302,** 1540.
[8] Tzallas, P., Charalambidis, D., Papadogiannis, N. A., Witte, K., and Tsakiris, G. D., 2003, *Nature,* **426,** 267
[9] Hentschel, M., Kienberger, R., Spielmann, Ch., Reider, G. A., Milosevic, N., Brabec, T., Corkum, P., Heinzmann, U., Drescher, M., and Karusz, F., 2001, *Nature,* **414,** 509.
[10] Wheatstone, C., 1835, *Phil. Mag.,* **6,** 61.
[11] Bradley, D. J., Liddy, B., and Sleat, W. E., 1971, *Opt. Commun.,* **2,** 391.
[12] Schelev, M. Ya, Richardson, M. C., and Alcock, A. J., 1971, *Appl. Phys. Lett.,* **18,** 354.
[13] Itatani, J., Quéré, F., Yudin, G. L., Ivanov, M. Yu, Klausz, F., and Corkum, P. B., 2002, *Phys. Rev. Lett.,* **88,** 173903.
[14] Kitzler, M., Milosevic, N., Scrinzi, A., Krausz, F., and Brabec, T., 2002, *Phys. Rev. Lett.,* **88,** 173904.
[15] Kienberger, R., Goulielmakis, E., Uiberacker, M., Baltuska, A., Yakovlev, V., Bammer, F., Scrinzi, A., Westerwalbesloh, Th., Kleineberg, U., Heinzmann, U., Drescher, M., and Krausz, F., 2004, *Nature,* **427,** 817.
[16] Kane, D. J., and Trebino, R., 1993, *IEEE J. quantum Electron.,* **29,** 571.
[17] Sekikawa, T., Katsura, T., Miura, S., and Watanabe, S., 2002, *Phys. Rev. Lett.,* **88,** 193902.
[18] Vampouille, M., Barthlmy, A., Colombeau, B., and Froehly, C., 1984, *J. Opt.* (Paris), **15,** 385.
[19] Kaufman, M. T., Banyai, W. C., Godil, A. A., and Bloom, D. M., 1994, *Appl. Phys. Lett.,* **64,** 270.
[20] Beck, M., Raymer, M. G., Walmsley, I. A., and Wong, V., 1993, *Opt. Lett.,* **18,** 2041.
[21] Walmsley, I., and Wong, V. J., 1996, *J. opt. Soc. Am.* B, **13,** 2453.
[22] Dorrer, Ch., and Kang, I., 2003, *Opt. Lett.,* **28,** 1481.
[23] Drescher, M., Hentschel, M., Kienberger, R., Uiberacker, M., Yakovlev, V., Scrinzi, A., Westerwalbesloh, Th., Kleineberg, U., Heinzmann, U., and Krausz, F., 2002, *Nature,* **419,** 803.

[24] L'Huillier, A., and Balcou, P., 1993, *Phys. Rev. Lett.,* **70,** 774.
[25] Macklin, J. J., Kmetec, J. D., and Gordon III, C. L., 1993, *Phys. Rev. Lett.,* **70,** 766.
[26] Schafer, K. J., Krause, J. L., and Kulander, K. C., 1992, *Int. J. nonlinear opt. Phys.,* **1,** 245.
[27] Schafer, K. J., Yang, B., DiMauro, L. F., and Kulander, K. C., 1993, *Phys. Rev. Lett.,* **70,** 1599.
[28] Corkum, P. B., 1993, *Phys. Rev. Lett.,* **71,** 1994.
[29] Lewenstein, M., Balcou, Ph., Ivanov, M., Yu, L'Huillier, A., and Corkum, P. B., 1994, *Phys. Rev.* A, **49,** 2117.
[30] Salières, P., Carré, B., Le Déroff, L., Grasbon, F., Paulus, G. G., Walther, H., Kopold, R., Becker, W., Milosevic, D. B., Sanpera, A., and Lewenstein, M., 2001, *Science,* **292,** 902.
[31] Christov, I. P., Murnane, M. M., and Kapteyn, H. C., 1997, *Phys. Rev. Lett.,* **78,** 1251.
[32] Kan, C., Burnett, N. H., Capjack, C. E., and Rankin, R., 1997, *Phys. Rev. Lett.,* **79,** 2971.
[33] de Bohan, A., Antoine, P., Milosevic, D. B., and Piraux, B., 1998, *Phys. Rev. Lett.,* **81,** 1837.
[34] Tempea, G., Geissler, M., and Brabec, T., 1999, *J. opt. Soc. Am.* B, **16,** 669.
[35] Seres, E., Seres, J., Krausz, F., and Spielmann, Ch., 2004, *Phys. Rev. Lett.,* **92,** 163002-1.